Chemical Science

ROYAL SOCIETY OF CHEMISTRY

EDGE ARTICLE

View Article Online
View Journal | View Issue

Cite this: *Chem. Sci.*, 2021, **12**, 3627

All publication charges for this article have been paid for by the Royal Society of Chemistry

In situ formation of a biomimetic lipid membrane triggered by an aggregation-enhanced photoligation chemistry†

Yaowu Zhou,‡[b] Huiting Yang,‡[b] Chenxi Wang,[b] Yuan Xue,[b] Xuebin Wang,[b] Chunyan Bao *[ab] and Linyong Zhu *[ab]

Received 3rd November 2020
Accepted 20th January 2021

DOI: 10.1039/d0sc06049f

rsc.li/chemical-science

Nature or synthetic systems that can self-assemble into biomimetic membranes and form compartments in aqueous solution have received extensive attention. However, these systems often have the problems of requiring complex processes or lacking of control in simulating lipid synthesis and membrane formation of cells. This paper demonstrates a conceptually new strategy that uses a photoligation chemistry to convert nonmembrane molecules to yield liposomes. Lysosphingomyelin (Lyso) and 2-nitrobenzyl alcohol derivatives (NBs) are used as precursors and the amphiphilic character of Lyso promotes the formation of mixed aggregates with NBs, bringing the lipid precursors into close proximity. Light irradiation triggers the conversion of NBs into reactive aldehyde intermediates, and the preassembly facilitates the efficient and specific ligation between aldehyde and Lyso amine over other biomolecules, thereby accelerating the synthesis of phospholipids and forming membrane compartments similar to natural lipids. The light-controllable transformation represents the use of an external energy stimulus to form a biomimetic phospholipid membrane, which has a wide range of applications in medicinal chemistry, synthetic biological and abiogenesis.

Introduction

Although life appeared on the earth as early as 3.5–4.0 billon years ago, it remains unclear how life originated under primitive conditions. Protocell models provide the possibility of analysing the mechanisms of the origin of life.[1–6] Cell membranes are considered a basic condition for the emergence of life, providing compartments for the formation of protocells, facilitating energy exchange with the outside world, and making metabolism and growth-division possible. To date, fatty acids,[7–9] simple amphiphiles[10,11] and phospholipids[12,13] have been proposed as plausible models of original cellular compartments, as they can spontaneously self-assemble into closed vesicles in water.

Compared to simple fatty acids and amphiphiles, phospholipids are often advantageous as models of primitive artificial cells due to their stability and similarity to modern cell membranes. Several methods have been developed for phospholipid synthesis from reactive precursors, which provide dynamic approaches for remodelling membranes and are powerful tools for origin-of-life research.[14–20] They can be simply divided into two types. One is based on the biomimetic catalytic coupling reactions between amphiphilic and non-amphiphilic precursors that drives the *in situ* self-assembly of lipid membranes.[14–17] However, the use of catalysts or additional ligands not only complicates the reaction system but also greatly impacts on its biocompatibility. The other is based on catalyst-free chemical coupling reactions to generate lipid membrane from nonmembrane-forming reactive precursors.[18–20] This process is spontaneous and lacks control, which is essentially different from the enzyme/energy-driven mechanism of native cell membrane production.[21] Therefore, it is of interest to develop catalyst-free and stimuli-responsive systems to synthesize membrane-forming lipids.[22]

Light represents an ideal energy supporter that drives many important processes in living systems.[23,24] Catalyst-free photochemical reactions provide alternative strategies to synthesize membrane-forming lipids. Recently, we have developed a photoligation chemistry in which 2-nitrobenzyl alcohol derivatives (NBs) can be converted into aldehyde intermediates upon light irradiation and then selectively coupled with amines.[25] Based

[a]*Optogenetics & Synthetic Biology Interdisciplinary Research Center, State Key Laboratory of Bioreactor Engineering, East China University of Science and Technology, 130# Meilong Road, Shanghai 200237, China. E-mail: baochunyan@ecust.edu.cn; linyongzhu@ecust.edu.cn*

[b]*Key Laboratory for Advanced Materials and Joint International Research Laboratory of Precision Chemistry and Molecular Engineering, Feringa Nobel Prize Scientist Joint Research Center, School of Chemistry and Molecular Engineering, East China University of Science & Technology, 130# Meilong Road, Shanghai, 200237, China*

† Electronic supplementary information (ESI) available: Synthesis, supplementary data and procedures: Fig, S1–S22; appendix of NMR and mass spectra of new compounds. See DOI: 10.1039/d0sc06049f

‡ These authors contributed equally.

on this photoligation chemistry, we herein describe the use for the synthesis of phospholipids from alkyl-substituted NBs and amine-containing lysosphingomyelin (Lyso) (Scheme 1a). As illustrated in Scheme 1b, the amphiphilic nature of Lyso enables it to form self-assembled aggregates with hydrophobic NBs in aqueous solution, which is conducive to promoting synthesis of phospholipids (**Lyso-NB**) by coupling the photogenerated aldehyde of NBs (**NBCHO**) with the amine of Lyso, thus driving the *in situ* formation of biomimetic liposomes. To demonstrate the ability as a biomimetic protocell model, guest molecule encapsulation, selective permeability and membrane-gated enzyme catalysis were explored, respectively.

Experimental section

Synthesis of compounds

See the details in ESI.†

Photoreaction characterizations

UV-vis absorption spectra and NMR spectra were used to track both of the photolysis and ligation processes in solutions, and high perform liquid chromatography (HPLC) and mass spectra were utilized to quantify the yields. See the details in ESI.†

Phototriggered formation of liposomes

100 μL NB (10 mM in $CHCl_3$) and 120 μL Lyso (10 mM in MeOH) was mixed in a glass vial and dried with N_2 stream to form a transparent film, which was further dried under vacuum overnight. 1 mL HEPES (10 mM, pH = 7.2) was added and vortexed to dissolve the film, the obtained mixture was cured in a shaker at 37 °C (90 rpm min^{-1}) for 5 h. Then, 20 μL of mixture was taken out and put on a glass slide for *in situ* microscopy observation. A LED 365 nm (20 mW cm^{-2}) was used to trigger the lipid synthesis and vesicle formation.

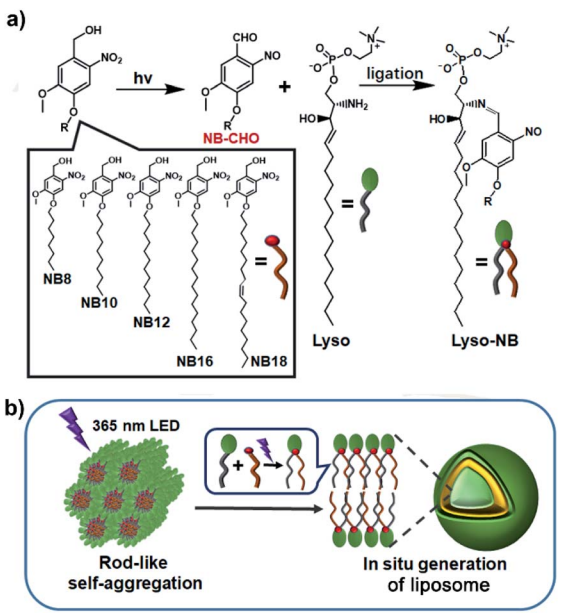

Scheme 1 Construction of liposomes. (a) The photoligation reactions from NB and Lyso precursors. (b) The proposed mechanism of the formation of liposome triggered by light irradiation.

HPTS dye encapsulation by the photogenerated liposomes

500 μL of a 10 mM solution of **NB10** in $CHCl_3$ and 600 μL of a 10 mM solution of lysosphingomyelin (Lyso) in MeOH were mixed in a glass tube and dried with N_2 stream to form a transparent film, which was further dried under vacuum overnight. Then, 1 mL HEPES buffer (10 mM, 150 mM NaCl, pH = 7.2) containing 1 mM HPTS was added and vortexed to dissolve the film, the obtained mixture was cured in a shaker at 37 °C (90 rpm min^{-1}) for 5 h. A LED 365 nm light with intensity of 10 mW cm^{-2} was used for vesicle formation. After irradiation, the obtained solution was analysed by flow cytometry to evaluate the encapsulation efficiency using an emission wavelength of 510 nm. Meanwhile, the encapsulated vesicles were investigated by confocal microscopy, in which the non-encapsulated dye was removed by size exclusion column chromatography (SephadexG-50) prior to the investigation.

The evaluation of membrane stability by tracking HPTS release

NB10/Lyso mixture was used as the sample. After encapsulation of HPTS as described above, the suspension was purified by size exclusion column chromatography (SephadexG-50) using HEPES buffer (10 mM, 150 mM NaCl, pH = 7.2) as eluent. The collected vesicles were diluted to reach a total lipid concentration of 1 mM, assuming 100% **NB10** was transferred into lipid. Then, 100 μL of above solution was transferred to a quartz cuvette followed by addition of 2900 μL of HEPES buffer (10 mM, 150 mM NaCl, pH = 7.2). The cuvette was placed in the fluorescence instrument with slow stirring condition by a magnetic stirrer equipped in the instrument (at t = 0 s). The time-dependent change in fluorescence intensity (λ_{em} = 510 nm) was monitored at an excitation wavelength at λ_{ex} = 450 nm, during the addition of base (30 μL, 0.5 M NaOH) at t = 100 s and Triton X-100 (60 μL, 5% aqueous solution) at t = 250 s.

In situ enzyme encapsulation and enzymatic cascade reaction

GOX–HRP enzymatic cascade reaction was selected as the model to explore the encapsulation and activity retention in photogenerated liposomes. The detailed encapsulation process was the same as that for HPTS, except 200 μL of glucose oxidase (600 U mL^{-1} in PBS) and 50 μL of horseradish peroxidase (400 U mL^{-1} in PBS) were added to the mixed buffer before light irradiation. After hydration and irradiation, the formed mixture was purified by size exclusion column chromatography (Sepharose 4B column (1.0 (id) × 30 cm)) using HEPES buffer as eluent.

Then, to 100 μL of collected vesicles was added 2900 μL HEPES and 10 μL of Amplex Red solution (1 mg mL^{-1} in DMSO). The obtained solution was detected by the fluorescence instrument with slow stirring condition by a magnetic stirrer equipped in the instrument (at t = 0 s). The time-dependent change in fluorescence intensity (λ_{em} = 585 nm) was

monitored at an excitation wavelength at $\lambda_{ex} = 571$ nm, during the addition of D-glucose (30 μL, 1.0 M in HEPES) at $t = 60$ s, alpha-hemolysin pore protein (α-HL, 100 μL, 250 μg mL^{-1} in HEPES) or Triton X-100 (60 μL, 5% in water) at $t = 120$ s. The system with the addition of glucose alone was used as a control to confirm the membrane barrier for the entrapped enzyme.

Results and discussion

A series of NBs compounds with different alkyl substituents, **NB8**, **NB10**, **NB12**, **NB16**, and **NB18** (Scheme 1a), were synthesized (details see ESI†) and a ligation product **Lyso-NB10** was prepared to quantify the yields of photoligation between Lyso and NBs (Fig. S1–S3†). Time-resolved UV-vis absorption of irradiated **NB10**/Lyso mixture in CH_3CN/H_2O (1 mM, v/v = 9/1) showed efficient and similar photolysis process as for **NB10** photolysis (Fig. S4 and S5†), which suggested that the imine-ligation was quite slow. Such a slow rate not only prevents light control for ligation, but also introduces the risk of side reactions from the aldehyde intermediate. Fortunately, a very different photoligation process occurred when the solvent was replaced with 4-(2-hydroxyethyl-1-piperazineethanesulfonic) acid buffer (HEPES, 10 mM, pH = 7.2). The ligation rate was significantly improved and almost no delay after light irradiation (Fig. S6†), revealing light controllability of the whole photoligation process. This control is attributable to the induced aggregation of the precursors, which greatly increased the ligation reactivity for the whole photoligation process. It is very useful and provides a premise for the *in situ* self-assembly of lipid membrane.

High perform liquid chromatography (HPLC) and mass spectra were further utilized to identify and quantify the reaction process, which exhibited results consistent with the above-described UV-vis analysis. As exhibited in Fig. 1a and b, the photolysis was almost completed upon 90 s irradiation in CH_3CN/H_2O (1 mM, v/v = 9/1), however, the ligation completed after 48 h culture in dark. In HEPES buffer, the irradiation induced the generation of **Lyso-NB10** immediately without appearance of aldehyde intermediate (**NBCHO**), and the yield of **Lyso-NB10** was approximately 62% (Fig. 1c and d). The relative low yield of photo-ligation should be attributed to the incomplete conversion of **NBCHO**, since *o*-nitrosobenzaldehyde was also sensitive to irradiation[25–27] and the amount of byproducts increased with the extension of irradiation time (Fig. S4b and c†). Tracking analysis showed that **NBCHO** was relatively stable in CH_3CN/H_2O and remained more than 90% after 48 h dark storage (Fig. S7†), which ensured the subsequent imine ligation reaction. However, **NBCHO** was not stable in water since there was no detectable **NBCHO** in HPLC profiles. Meanwhile, the photolysis time in HEPES was significantly increased (25 min irradiation) due to the bad solubility of **NB10**. It is also suggested that the generation of **Lyso-NB10** should be attributed to the preassembly of precursors in HEPES, in which Lyso provided a hydrophobic environment for **NB10** to form **NBCHO** and couple with Lyso immediately.

A photoresponsive compound **17** which can photogenerate ketone was used as a contrast for the photoreaction with **NB10**. No detectable ligation product indicated the importance of **NBCHO** for the synthesis of lipids (Fig. S8†). The photoligation was also carried out in the presence of other amine-containing substances (Table 1, Fig. S9 and S10†). The results showed that the yield of lipid was unaffected and that the added amino acids (except for the cysteine) and proteins do not participate in the photoligation reaction. It should also be attributed to the formation of aggregates between the precursors, thus accelerating lipid synthesis rather than reacting with other amine molecules in aqueous solution. It is very important as a candidate for mimicking natural membrane generation. Aggregation induced ligation reaction also helps to overcome the effect of pH, and the ligation yields are comparable in buffers at various pH (pH = 5, 7.2, 10, respectively, Table 1). Since traditional imine products are always pH-sensitive and reversible, the stability of **Lyso-NB10** was explored. It exhibited that **Lyso-NB10** was quite stable under neutral and alkaline conditions, however, it was labile in acidic condition and the amount

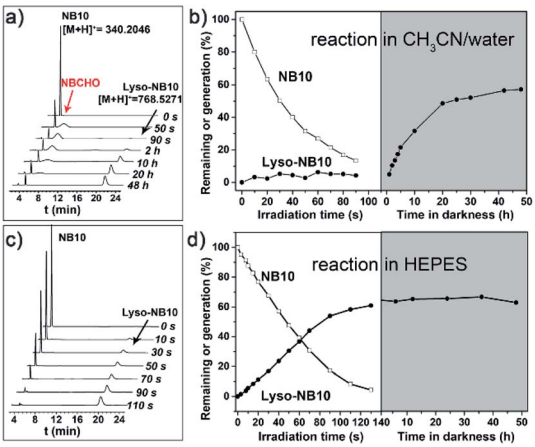

Fig. 1 Quantitative analysis of photoligation. (a and c) Time-resolved partial HPLC spectra and (b and d) the corresponding amounts of NB10 remaining (-□-) and Lyso-NB10 generation (-●-) during the photoligation process of the NB10/Lyso mixture in different solvents. (a and b) 1/1.2 mM in CH_3CN/water (v/v = 9/1), (b and d) 1/1.2 mM in HEPES solution (10 mM, pH = 7.2). A LED with an emission wavelength of 365 nm and an intensity of 10 mW cm^{-2} was used.

Table 1 Effect of reaction conditions on photoligation of NB10/Lyso mixture under LED 365 nm irradiation

Conditions	Yield of **Lyso-NB10**
Tris-buffer, pH = 5.0	58%
HEPES, pH = 7.2	62%
Borate buffer, pH = 10.0	64%
1 mM lysine	60%
1 mM glutamate	65%
1 mM serine	61%
1 mM cysteine	50%[a]
10 mg mL^{-1} BSA	61%

[a] The presence of cysteine decreased the photoligation yield of **Lyso-NB10**, however, no stable ligation product between **NB10** and cysteine was detected from the HPLC trace analysis.

reduced ~30% after 24 h storage (Fig. S11†). The photoligation between other NBs and Lyso in HEPES suggested that the length of the hydrophobic chain of NBs affected lipid synthesis (Fig. S12†), with the shorter ones being beneficial to lipid synthesis (~65% **Lyso-NB8**, ~44% **Lyso-NB12**, ~33% **Lyso-NB16** and ~46% **Lyso-NB18**, respectively). The different ligation yield can be explained by following self-assembly study.

To verify above aggregation-induced role, the self-assembling properties of the precursors in HEPES were explored. Accordingly, **NB8**/Lyso produced needle-like precipitates, **NB10**/Lyso, **NB12**/Lyso and **NB16**/Lyso formed white suspensions, and **NB18**/Lyso yielded a translucent emulsion (Fig. S13†). Except for **NB18**/Lyso, all the precursors exhibited similar rod-like aggregates in HEPES (Fig. 2a, b, S14†). Small angle X-ray diffraction (SAXD) data (Fig. 2c) indicated that **NB10**/Lyso formed the long-range ordered structure of hexagonal columnar stacking (reciprocal d-spacing of $1 : \sqrt{3} : 2$) with $a = 2.8$ nm. Israelachvili *et al.* showed that amphiphilic molecules with a packing parameter $0.3 < P < 0.5$ ($P = V/a_0 l_c$) self-assembled into cylindrical micelles.[28] It was reasonable to speculate that Lyso encapsulates **NB10** molecules to self-assemble into cylindrical micelles that arrange in parallel into hexagonal stacking (inset of Fig. 2c). The different aggregation of **NB18**/Lyso in HEPES should be attributed to the extension of hydrophobic tails of NBs, which induced the increase in P and vesicle self-assembly ($P > 0.5$). Based on the different assembly morphology, from the long and rigid rod-like crystals of **NB8**/Lyso to the short and soft rod-like aggregates of **NB16**/Lyso, it was reasonable to speculate that the higher ligation yield of NB/lyso mixtures with shorter hydrophobic chains should be due to the more compact molecular stacking (as the highest yield of **Lyso-NB8**). For comparison, the self-assembled morphologies of **NB10** and Lyso were explored. As expected, **NB10** exhibited amorphous structures due to the insolubility in HEPES and Lyso formed micelles in HEPES, respectively (Fig. S15†). It indicated that the rod-like aggregates of **NB10**/Lyso resulted from the coassembly of precursors. A surfactant, hexadecyl trimethyl ammonium bromide (CTAB), was also added to disrupt the NB/Lyso assembly. The decreased ligation yield of **Lyso-NB10** (around 45%, Fig. S16†) further confirmed the importance of preassembly for subsequent imine ligation reaction between aldehyde and amine. All these findings confirmed that the NBs and Lyso self-assembled in HEPES, which accelerated the imine ligation and resulted in specific, efficient and light-controllable lipid synthesis.

Then, the dynamics of lipid vesicles generation were explored. As illustrated in Fig. 3a, upon irradiation of the **NB10**/Lyso mixture, the rod-like aggregates gradually converted into vesicles (Movie S1†). The transition occurred rapidly, completing within 1 min, and the generated vesicles were stable in HEPES (more than 7 days at 0–4 °C) with diameter of 0.2–1 μm (Fig. 3b and c). Hollow vesicle structure can also be verified by the fluorescent image of some large vesicles with addition of Nile red dye (Fig. S17†). SAXD analysis (Fig. 3d) revealed the bilayer stacking of the vesicles, with a period of 4.44 nm, comparable to those of natural liposomes. To rule out the effect of temperature during the illumination process, the temperature was tracked throughout the irradiation process and the change was ignorable. In addition, thermal-induced transformation is always reversible; for example, rod-like aggregates

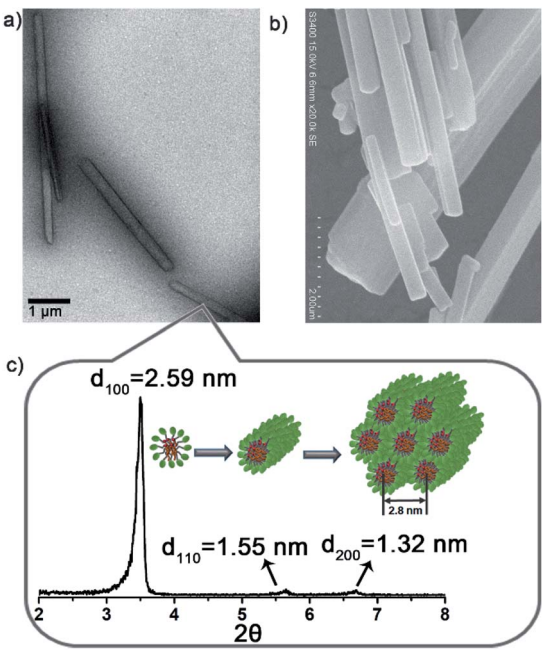

Fig. 2 Self-assembly analysis of the **NB10**/Lyso mixture in HEPES (1/1.2 mM). (a) TEM and (b) SEM images of the aggregates. (c) SAXD diagrams of the rod-like aggregates. Inset shows the proposed stacking model of the aggregates.

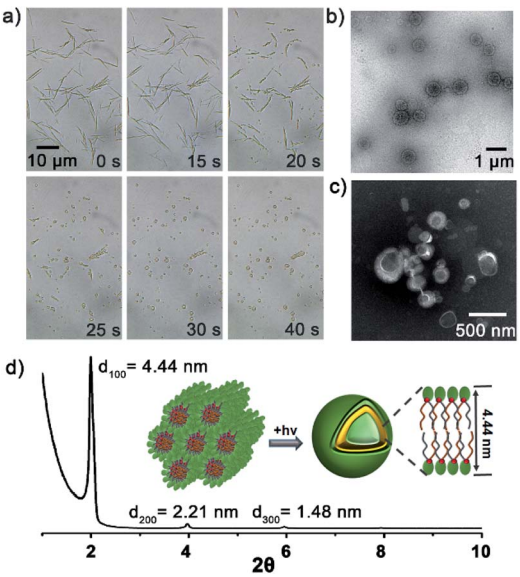

Fig. 3 *In situ* formation of bilayer vesicles. (a) Microscopy images of the dynamic generation of lipid vesicles from **NB10**/Lyso aggregates triggered by light. A LED with an emission wavelength of 365 nm and an intensity of 10 mW cm^{-2} was used for irradiation. (b and c) TEM images of the vesicles; those in (c) were negatively stained by phosphotungstic acid. (d) SAXD diagrams of the **Lyso-NB10** liposomes generated by photoligation.

of **NB10**/Lyso can be converted into vesicles reversibly by controlling the temperature (Fig. S18†). It confirmed that the formation of the stable bilayer vesicles was triggered by the photoligation chemistry. Similar to the **NB10**/Lyso mixture, the **NB8**/Lyso and **NB12**/Lyso mixtures exhibited the transition to vesicles upon irradiation (Fig. S19, Movie S2 and S3†). However, the **NB16**/Lyso mixture exhibited collapse of rod aggregates and finally formed sheet-like aggregates upon irradiation (Fig. S20†), which might have been related to its low lipid yield (33% for **Lyso-NB16**). The irradiation of **NB18**/Lyso mixture did not cause any change in morphology since it had already formed vesicle aggregates before irradiation (Fig. S21†).

To confirm the membrane compartments of the vesicles, a water-soluble fluorophore, 8-hydroxyprene-1,3,6-trisulfonic acid (HPTS), was added to a mixture of **NB10**/Lyso aggregates in HEPES. The light-triggered generation of fluorescent vesicles, as illustrated in Fig. 4a, confirmed the successful encapsulation of HPTS. Neither vesicle nor encapsulation was observed for **NB10** and Lyso alone. Flow cytometry (Fig. 4b) illustrated that the irradiated mixture exhibited significantly enhanced fluorescence compared to that of the control sample (**NB18**/Lyso mixture without irradiation), indicating membrane compartmentalization and reassembly for HPTS encapsulation in the cavity. The encapsulation efficiency was consistent with the lipid yields, with **NB16**/Lyso exhibiting the poorest performance. After removing the unencapsulated HPTS, the stability of the membrane was evaluated by tracking the pH-induced changes in HPTS fluorescence (Fig. S22†). The results showed that the fluorescence of HPTS at 510 nm did not change with the addition of base, which proved membrane barrier and stability, and showed typical characteristics of lipid membranes.

Finally, to explore whether the generated membrane can mimic the key features of biological membranes, for example, bioreactor capacity, a glucose oxidase (GOX)–horseradish peroxidase (HRP) enzymatic cascade reaction was used with the **NB10**/Lyso system. In such a cascade reaction, two enzyme mediated steps are involved: (1) GOX oxidizes glucose to produce hydrogen peroxide; (2) HRP catalysts Amplex Red to produce fluorescent resorufin in the presence of hydrogen peroxide.[29,30] Therefore, the enzymes' activity in liposomes can be evaluated by tracking the conversion of red-fluorescent resorufin at 585 nm (λ_{ex} = 571 nm). As illustrated in Fig. 4c, GOX and HRP were encapsulated in the photogenerated liposomes by illumination and removal of the excess enzyme, and then Amplex Red was added outside the vesicles. Amplex Red is a neutral molecule, which can freely transmit across the lipid bilayer wall and enter into the aqueous interior of liposomes.[30–32] The change in fluorescence intensity with time was monitored during the addition of β-D-glucose and other membrane-active components. Fig. 4d illustrated that the fluorescence changed little when only glucose was added. It indicated that glucose could not diffuse into vesicles to initiate enzyme cascade reaction. Then, a membrane pore protein α-hemolysin was added, which spontaneously inserted into bilayers and allowed glucose diffusion into the vesicle through the pores. As a result, the GOX–HRP enzymatic cascade reaction was initiated and yielded a significant increase in fluorescence as well as a rapid increase by the addition of Triton X-100 (Fig. 4d and S23†). These findings suggested that the photogenerated liposome membrane provided an effective and stable barrier for enzyme molecules and demonstrated its ability to be used as a bioreactor.

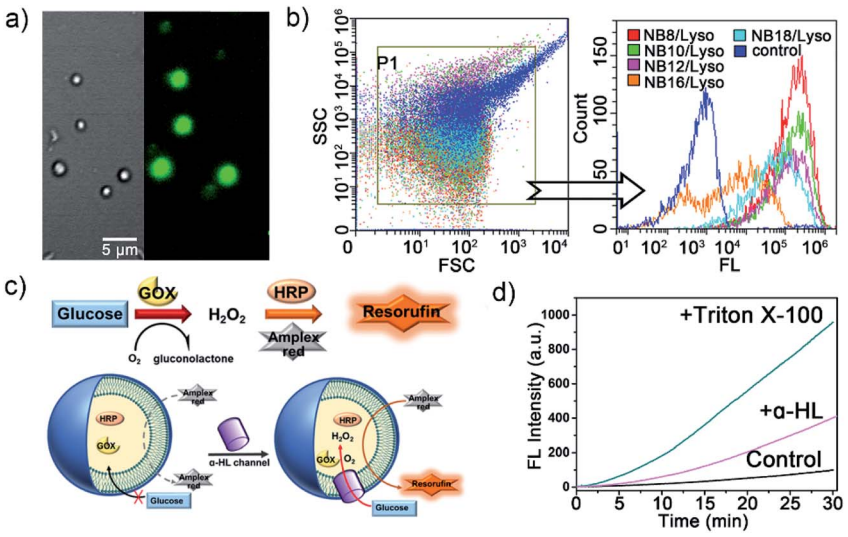

Fig. 4 Compartmentalization formation as biomimetic membranes. (a) Bright field (left) and fluorescent (right) confocal microscopy images of HPTS-entrapped vesicles generated by irradiating **NB10**/Lyso aggregates in HPTS-contained buffer. (b) Flow cytometry analysis of HPTS entrapped vesicles; **NB18**/Lyso aggregates in HPTS-contained buffer without irradiation were used as the control sample. (c) Schematic of the GOX–HRP enzymatic cascade reaction and the mechanism involving the membrane-forming compartments. (d) The evolution of fluorescence intensity of resorufin during the period of cascade reaction. "+Triton X-100" and "+α-HL" denote the addition of Triton X-100 and α-HL, respectively. "Control" denotes no additional channel or detergent molecules.

Conclusions

In summary, we have developed a nonenzymatic photoligation chemistry for the *de novo* synthesis of phospholipid membranes. The aggregation of precursors enabled high specificity and efficient production of lipid without being affected by other coexisting biomolecules, facilitating the formation of membrane-bound liposomes. The successful entrapment of enzyme and the occurrence of the GOX–HRP enzymatic cascade initiated by glucose transmembrane transport proved the applicability of the phototriggered liposomes as bioreactors. This approach represents the first example of the formation of phospholipid membrane using a catalysis-free photoligation chemistry and represents an advance in the mimicry of the compartmentalization of cells.

Author contributions

C. Bao proposed and supervised the project. Y. Zhou and H. Yang carried out the synthesis, characterizations and data collection. C. Wang, Y. Xue, and X. Wang performed the experiments of dye encapsulation and enzyme cascade reaction. C. Bao and L. Zhu oversaw the paper with edits from all authors. All the authors discussed the results and commented on the manuscript.

Conflicts of interest

There are no conflicts to declare.

Acknowledgements

This work is supported by the National Key Research and Development Project (2019YFA0110500) and NSFC (Grant No. 21472044). The authors thank Research Centre of Analysis and Test of East China University of Science and Technology for the help on the characterizations.

Notes and references

1 J. W. Szostak, D. P. Bartel and P. L. Luisi, *Nature*, 2001, **409**, 387.
2 E. Rideau, R. Dimova, P. Schwille, F. R. Wurm and K. Landfester, *Chem. Rev.*, 2018, **47**, 8572.
3 I. Insua and J. Montenegro, *Chem*, 2020, **6**, 1.
4 X. Wang, X. Liu and X. Huang, *Adv. Mater.*, 2020, **32**, 2001436.
5 Y. Qiao, M. Li, R. Booth and S. Mann, *Nat. Chem.*, 2017, **9**, 110.
6 A. F. Mason, N. A. Yewdall, P. L. W. Welzen, J. Shao, M. van Stevendaal, J. C. M. van Hest and D. S. Willams, *ACS Cent. Sci.*, 2019, **5**, 1360.
7 P. Walde, R. Wick, M. Fresta, A. Mangone and P. L. Luisi, *J. Am. Chem. Soc.*, 1994, **116**, 11649.
8 T. F. Zhu and J. W. Szostak, *J. Am. Chem. Soc.*, 2009, **131**, 5705.
9 A. E. Engelhart, K. P. Adamala and J. W. Szostak, *Nat. Chem.*, 2016, **8**, 448.
10 D. Garenne, L. Beven, L. Navailles, F. Nallet, E. J. Dufourc and J. P. Douliez, *Angew. Chem., Int. Ed.*, 2016, **55**, 13475.
11 R. J. Brea, A. Bhattacharya, R. Bhattacharya, J. Song, S. K. Sinha and N. K. Devaraj, *J. Am. Chem. Soc.*, 2018, **140**, 17356.
12 A. Bhattacharya, R. J. Brea and N. K. Devaraj, *Chem. Sci.*, 2017, **8**, 7912.
13 K. Kurihara, M. Tamura, K. Shohda, T. Toyota, K. Suzuki and T. Sugawara, *Nat. Chem.*, 2011, **3**, 775.
14 C. Y. Zhou, H. Wu and N. K. Devaraj, *Chem. Sci.*, 2015, **6**, 4365.
15 M. D. Hardy, J. Yang, J. Selimkhanov, C. M. Cole, L. S. Tsimring and N. K. Devaraj, *Proc. Natl. Acad. Sci. U. S. A.*, 2015, **112**, 8187.
16 M. S. DeClue, P.-A. Monnard, J. A. Bailey, S. E. Maurer, G. E. Collis, H.-J. Ziock, S. Rasmussen and J. M. Boncella, *J. Am. Chem. Soc.*, 2009, **131**, 931.
17 M. Hardy, D. Konetski, C. Bowman and N. K. Devaraj, *Org. Biomol. Chem.*, 2016, **14**, 5555.
18 C. B. Minkenberg, F. Li, P. van Rijn, L. Florusse, J. Boekhoven, M. C. Stuart, G. J. Koper, R. Eelkema and J. H. van Esch, *Angew. Chem., Int. Ed.*, 2011, **50**, 3421.
19 C. A. Zentner, F. Anson, S. Thayumanavan and T. M. Swager, *J. Am. Chem. Soc.*, 2019, **141**, 18048.
20 R. J. Brea, C. M. Cole and N. K. Devaraj, *Angew. Chem., Int. Ed.*, 2014, **53**, 14102.
21 A. Yamashita, T. Sugiura and K. Waku, *J. Biochem.*, 1997, **122**, 1.
22 A. Bhattacharya, R. J. Brea, H. Niederholtmeyer and N. K. Devaraj, *Nat. Commun.*, 2019, **10**, 300.
23 F. D. Maria, F. Lodola, E. Zucchetti, F. Benfenati and G. Lanzani, *Chem. Soc. Rev.*, 2018, **47**, 4757.
24 J. W. Hindley, Y. Elani, C. M. McGilvery, S. Ali, C. L. Bevan, R. V. Law and O. Ces, *Nat. Commum.*, 2018, **9**, 1093.
25 C. Wang, Y. Liu, C. Bao, Y. Xue, Y. Zhou, D. Zhang, Q. Lin and L. Zhu, *Chem. Commun.*, 2020, **56**, 2264.
26 M. Gaplovsky, Y. V. Il'ichev, Y. Kamdzhilov, S. V. Kombarova, M. Mac, M. A. Schwörer and J. Wirz, *Photochem. Photobiol. Sci.*, 2005, **4**, 33.
27 Y. V. Il'ichev, M. A. Schwörer and J. Wirz, *J. Am. Chem. Soc.*, 2004, **126**, 4581.
28 J. N. Israelachvili, D. J. Mitchell and B. W. Ninham, *J. Chem. Soc., Faraday Trans. 2*, 1976, **72**, 1525.
29 H. H. Gorris and D. R. Walt, *J. Am. Chem. Soc.*, 2009, **131**, 6277.
30 Y. Elani, R. V. Law and O. Ces, *Nat. Commun.*, 2014, **5**, 5305.
31 M. Gosoy-Gallardo, C. Labay, V. D. Trikalitis, P. J. Kempen, J. B. Larsen, T. L. Andresen and L. Hosta-Rigau, *ACS Appl. Mater. Interfaces*, 2017, **9**, 15907.
32 L. Hosta-Rigau, M. J. York-Duran, Y. Zhang, K. N. Goldie and B. Städler, *ACS Appl. Mater. Interfaces*, 2014, **6**, 12771.